

UK Carbon Capture and Storage Demonstration Competition

UKCCS - KT - S7.21 - Shell - 001
PVT Report

April 2011
ScottishPower CCS Consortium

UK Carbon Capture and Storage Demonstration Competition

UKCCS - KT - S7.21 - Shell - 001
PVT Report

April 2011

ScottishPower CCS Consortium

IMPORTANT NOTICE

Information provided further to UK Government's Carbon Capture and Storage ("CCS") competition to develop a full-scale CCS facility (the "Competition")

The information set out herein (the **Information**) has been prepared by ScottishPower Generation Limited and its sub-contractors (the **Consortium**) solely for the Department for Energy and Climate Change in connection with the Competition. The Information does not amount to advice on CCS technology or any CCS engineering, commercial, financial, regulatory, legal or other solutions on which any reliance should be placed. Accordingly, no member of the Consortium makes (and the UK Government does not make) any representation, warranty or undertaking, express or implied as to the accuracy, adequacy or completeness of any of the Information and no reliance may be placed on the Information. In so far as permitted by law, no member of the Consortium or any company in the same group as any member of the Consortium or their respective officers, employees or agents accepts (and the UK Government does not accept) any responsibility or liability of any kind, whether for negligence or any other reason, for any damage or loss arising from any use of or any reliance placed on the Information or any subsequent communication of the Information. Each person to whom the Information is made available must make their own independent assessment of the Information after making such investigation and taking professional technical, engineering, commercial, regulatory, financial, legal or other advice, as they deem necessary.



PVT Modelling Report for CO₂ in Goldeneye Project

Table of Contents

| | |
|-------------------------------------|----|
| 1. INTRODUCTION | 3 |
| 2. EXECUTIVE SUMMARY | 3 |
| 3. PVT DATA AVAILABLE | 4 |
| 4. PVT CHARACTERISATION | 7 |
| 5. PVT LUMPING SCHEME | 12 |
| 6. CO ₂ FLUID PROPERTIES | 17 |
| 7. CONCLUSION | 22 |
| 8. ABBREVIATIONS | 23 |

Tables

| | |
|--|----|
| Table 3-1 History of PVT Characterisations | 5 |
| Table 8-1 Well name abbreviations | 23 |

Figures

| | |
|---|----|
| Figure 3-1 Goldeneye field top structure map showing well locations | 4 |
| Figure 3-2 Representative Goldeneye recombined gas compositions from exploration, appraisal and development wells. | 6 |
| Figure 3-3 Representative Goldeneye well phase envelopes from exploration, appraisal and development wells. | 6 |
| Figure 4-1 Retrograde condensate %VDp match of CVD data with full characterisation | 8 |
| Figure 4-2 Cumulative % volume of the initial wellstream produced. Match of CVD data with full characterisation | 8 |
| Figure 4-3 Gas viscosity (calculated) match of CVD data with full characterisation | 9 |
| Figure 4-4 Gas compressibility Z-factor match of CVD data with full characterisation | 9 |
| Figure 4-5 Retrograde condensate %VDp match of CME data with full characterisation | 10 |
| Figure 4-6 Relative volume match of CME data with full characterisation | 10 |
| Figure 4-7 Gas deviation Z-factor match of CME data with full characterisation | 11 |
| Figure 5-1 Example pseudoisation procedure reducing an original EOS characterisation with 22 components to multiple pseudoised characterisations [from Whitson, 1999] | 13 |
| Figure 5-2 Changes in the phase envelope during the stepwise pseudoisation | 14 |
| Figure 5-3. Changes in the retrograde condensate % (Vd) during the stepwise pseudoisation | 14 |
| Figure 5-4. Gas viscosity before and after regressing over the critical volume | 15 |
| Figure 5-5. GYA03 fluid composition before and after lumping | 16 |
| Figure 6-1. Phase diagram of CO ₂ [from Wong, 2005] | 17 |
| Figure 6-2. CO ₂ Density and Viscosity as a function of pressure. NIST data vs. PVTsim PR78P EOS | 18 |



| | |
|--|----|
| Figure 6-3. CO ₂ density error function versus pressure (psia) for a range of temperatures | 19 |
| Figure 6-4. CO ₂ Viscosity error function versus pressure (psia) for a range of temperatures | 19 |
| Figure 6-5. CO ₂ density comparison among NIST and different volume shift values (Cpen) for PR78 Peneloux EOS | 20 |
| Figure 6-6. CO ₂ Density error function versus pressure (psia) for a range of Cpen values | 21 |
| Figure 6-7. CO ₂ viscosity comparison among NIST and different volume shift values (Cpen) for PR78 Peneloux EOS | 21 |
| Figure 6-8. CO ₂ Viscosity error function versus pressure (psia) for a range of Cpen values | 22 |



1. Introduction

This report details the PVT characterisation that will be used to model the phase behaviour of CO₂ injection into the depleted Goldeneye Gas Condensate field.

The report includes the following:

- Preparation of a consistent Equation of State compositional model for Goldeneye Gas Condensate PVT. This involves the rationalisation of hydrocarbon single components (lumping) to achieve a representative but at the same time manageable fluid characterisation.
- Representation of CO₂ properties through an Equation of State.
- Summary of PVT samples available from Goldeneye
- Discussion of lumping, validation plots (full PVT) and 6 components (lumped)
- CO₂ Phase behaviour representation from Peng-Robinson EOS

Reference to third party software in this document is solely for information purposes to assist in understanding how the work was completed, does not amount to an endorsement of that software nor is any warranty as to its suitability given or implied.

2. Executive Summary

The Goldeneye hydrocarbon reservoir fluids have been extensively characterised during the hydrocarbon production phase of the fields. This PVT characterisation has been updated and extended to facilitate (i) an equation of state description in the reservoir simulation, (ii) a good representation of the properties of CO₂ at storage conditions.



3. PVT data available

In 1996 Shell discovered the Goldeneye field by drilling well 14/29a-3 and finding a gas column of 303ft. In the following years three appraisal wells were drilled: 1998 Amerada 20/4b-6 (South), 1999 Shell 14/29a-5 (South-East) and 2000 Amerada 20/4b-7 (South-West).

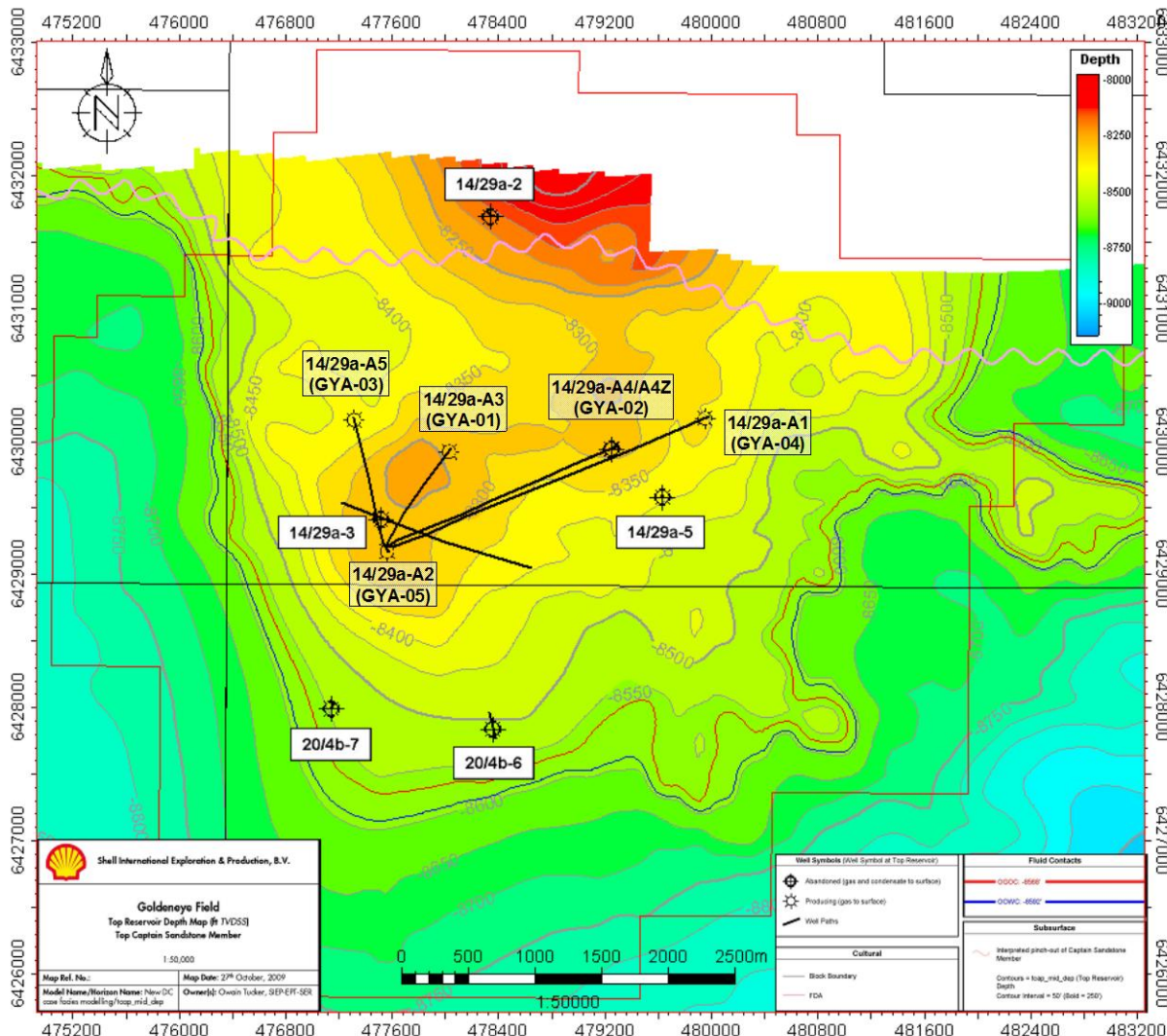


Figure 3-1 Goldeneye field top structure map showing well locations

In 2004 five development wells were drilled. The locations of the exploration and development wells are shown in Figure 3-1.

Fluid samples were taken from all four discovery/appraisal wells during RFT/MDT tests and surface samples from DST tests. PVT samples were taken from the test separator during clean up of the five Goldeneye development wells (GYA01 to GYA05). Detailed analysis from two of the wells was carried out, GYA04 and GYA03, including geochemical analysis. Gas and liquid compositions were determined for the other wells.

The complete list of PVT samples available from Goldeneye is shown in Table 3-1 below:



History of PVT Characterizations

MDT

| DST | Well | sample | Contents | Characterization | Well | sample | Contents | Characterization |
|-----|----------|---|---------------------------------|---|----------|--|---|---|
| | 14/29a-3 | 2336-C1-F 2781-M1-F | gas liq } | Gas & Liq comp, RC,CCE, CVD | 14/29a-3 | 313415 (*) 120085(*) 120083 312104 Atmospheric | gas & Liquid oil drilling fluid & water drilling fluid & water FP | FP, FLS, Gas Comp FP, CCE, FLS, RC drilling fluid & water FP, water analysis drilling fluid & water FP, water analysis FP |
| | 20/4b-6 | 1744-M1-F 4309-C1-F 3458-M1-F 1422-M1-F 4380-M1-F | gas gas liq gas liq | Comp, FLS, RC Comp, FLS, RC Comp, FLS, RC Comp, FLS, RC Comp, FLS, RC | 1429a-3 | 3452-M1-F(**) | oil | RC, CCE, DV, V |
| | | | | | 204b-6 | 0301-G1-F | oil | FLS, Liq comp, fluid prop, CCE, DV, V analysis |
| | | | | | | 9882-B1-F 3078-G1-F | water water | analysis |
| | | | | | | 37(*) 56(***) 554(*) | gas gas oil | FP, Gas Comp Gas Comp FP, Comp, FLS, prop, CCE, DV analysis |
| | | | | | | 550 & 535 | water | |
| | GYA04 | 1896-M1-F 5064-M1-F | gas liquid | Gas & Liq Comp, RC, CCE, CVD MSST | 14/29a-5 | | | |
| | GYA03 | 3263-M1-F 2193-C1-F 2188-M1-F | | | | | | |
| | GYA01 | 2766-M1-F 2191-C1-F 0917-M1-F | | Gas & Liq comp | | | | |
| | GYA02 | 3329-C1-F 0760-M1-F | | Gas & Liq comp | | | | |
| | GYA05 | 0966-M1-F 2726-C1-F 2389-M1-F | | Gas & Liq comp | | | | |

Multi-Stage Separator Test

| Well | well head | sample | Contents | Characterization | FP | Fingerprint analysis |
|----------|-----------|---------------------|----------|---|------|--------------------------------|
| 14/29a-3 | | 1-24 (2846-S1-F) | Gas | Gas Comp Recombined | FLS | Flash to standard conditions |
| | | 1-26 (3189-S1-F) | Gas | Gas Comp, Multi stage sep test | CCE | Constant Composition Expansion |
| | | 1-27 (3615-S1-F) | Gas | Gas Comp, Comp from flash at J/T conditions | DV | Differential Vapourisation |
| | separator | sample (DST) | Contents | Comments | CVD | Constant Volume Depletion |
| 14/29a-3 | | 1-3 (1349-C1-F)**** | Gas | (*) Contamination from FP analysis | V | Viscosity |
| | | 1-4 (2674-C1-F) | Gas | (**) Transferred from 120085, initial FP analysis showed | SF | Separator flash |
| | | 1-2 (1648-M1-F) | liquid | that the sample was slightly contaminated with drilling fluid base oil. | RC | Recombination |
| | | | | (***) Low volume of sample, insufficient liquid produced during flash | MSST | Multi stage separator test |
| | | | | separation for analysis, gas comp not representative | | |
| | | | | (****) low pressure reported on opening | | |
| | | | | Samples used for PVT characterisation of Goldeneye | | |

Table 3-1 History of PVT Characterisations

Some of these samples were identified as non-representative of Goldeneye fluids. The finger print analysis indicated contamination. There are sufficient representative fluid samples covering the hydrocarbon column and well spread across the field through the development wells (GYA01 to GYA05), to give confidence in the final characterisation.

Figure 3-2 and Figure 3-3 below presents recombined gas compositions and phase envelopes from all exploration, appraisal and development wells considered representative.



Goldeneye Recombined Gas Compositions

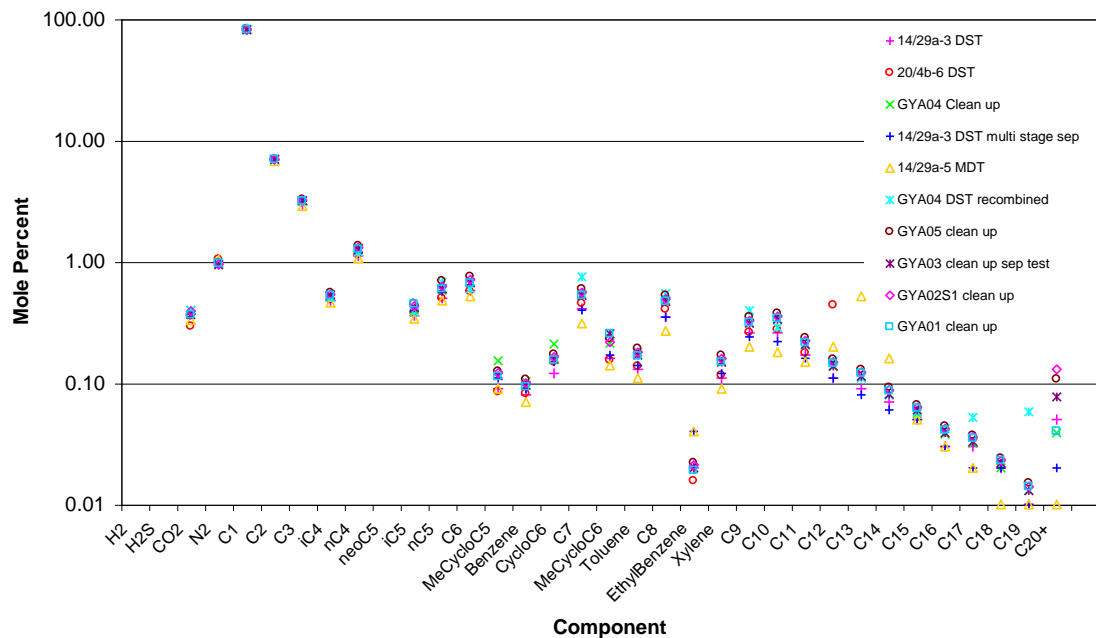


Figure 3-2 Representative Goldeneye recombined gas compositions from exploration, appraisal and development wells.

Goldeneye Well Phase Envelopes

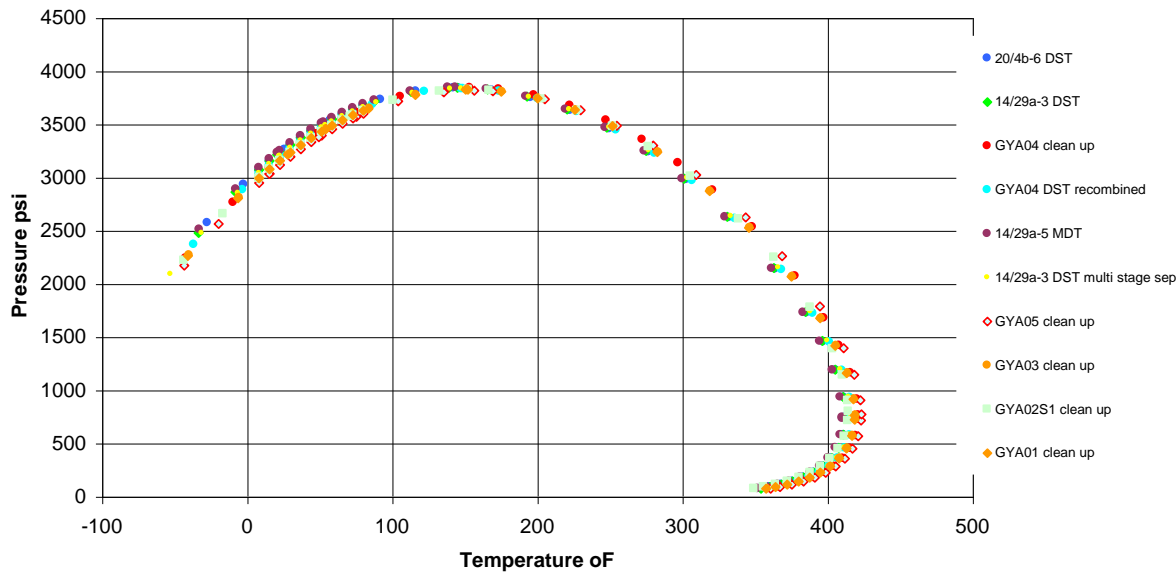


Figure 3-3 Representative Goldeneye well phase envelopes from exploration, appraisal and development wells.

Figure 3-2 shows all the valid recombined gas composition samples illustrating that compositionally all the gas samples exhibit a high degree of consistency. The phase envelope in Figure 3-3 of all the valid samples again illustrates the similarity between all the different samples.

Taking this into account and considering that only GYA03 and GYA04 have a complete PVT suite of experiments, the PVT model currently used by Shell for modelling full field and forecasting was generated based on the surface sample of well GYA03. Both GYA03 and GYA04 data were matched against the experimental Constant Mass Expansion (CME) and Constant Volume Depletion (CVD) data. 14/29a-3 was also matched for completeness.

4. PVT Characterisation

The PVT characterisation used for the current Goldeneye field full field dynamic modelling was re-run using a recent release of the PVT modelling software (PVTsim version 17.3 from CALSEP)¹. This was needed in order to facilitate the subsequent PVT lumping step. There were no changes apparent in moving to the newer version of the software.

In order to achieve a coherent fluid characterisation for Goldeneye, a typical workflow for a gas condensate was followed. It involved:

- Normal regression to tune to general phase behaviour (saturation pressure, CVD and CME observations). Not attempting to get a perfect match since the subsequent lumping process would change the match.
- Grouping/lumping components to reduce simulation time while retaining the predictability of the EOS.
- Fine tuning regression choosing high weights on experiments or observations (Saturation Pressure, Retrograde Condensate %, etc.) to improve the match of key data, and finally,
- Matching viscosity data while decoupling the rest of the experiments, regressing on the critical volume for each component's contribution to the total viscosity.

The Equation of State (EOS) used was Peng-Robinson 78 (PR78) Peneloux². The sample was adjusted to a saturation point of 3815 psia [~ 263 bara] at a reservoir temperature of 181°F [82.78°C]. The following plots compare the results from the tuned EOS model and the experimental data. Note that the reservoir abandonment pressure is in the neighbourhood of 2200 psia [~ 151 bara].

¹ Reference to third party software in this document is solely for information purposes to assist in understanding how the work was completed, does not amount to an endorsement of that software nor is any warranty as to its suitability given or implied.

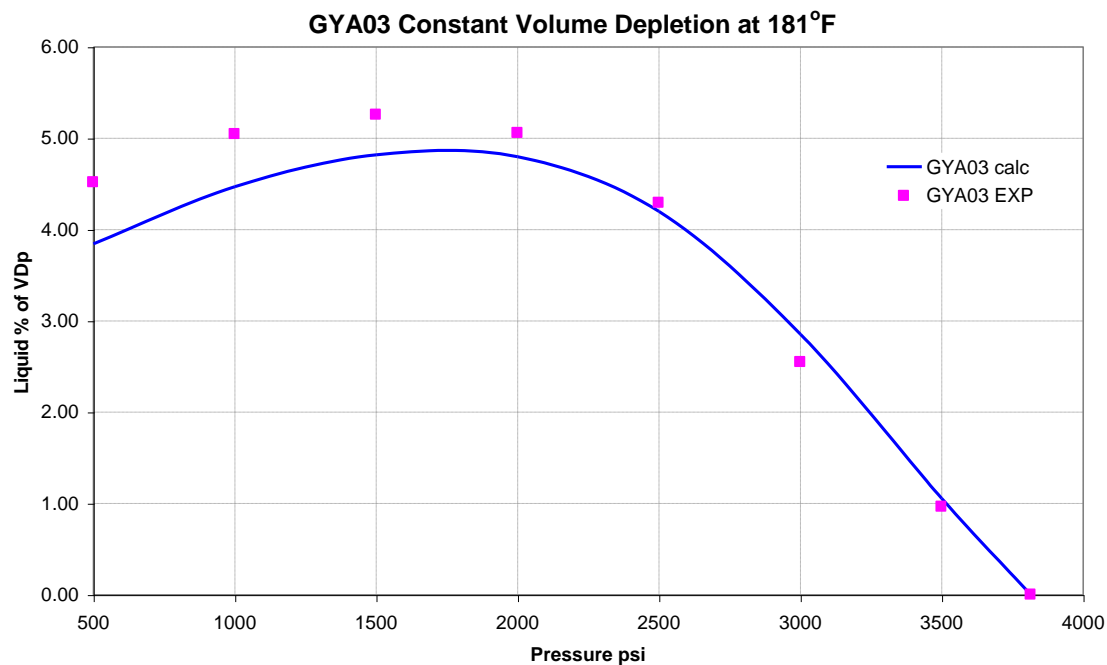


Figure 4-1 Retrograde condensate %VDp match of CVD data with full characterisation

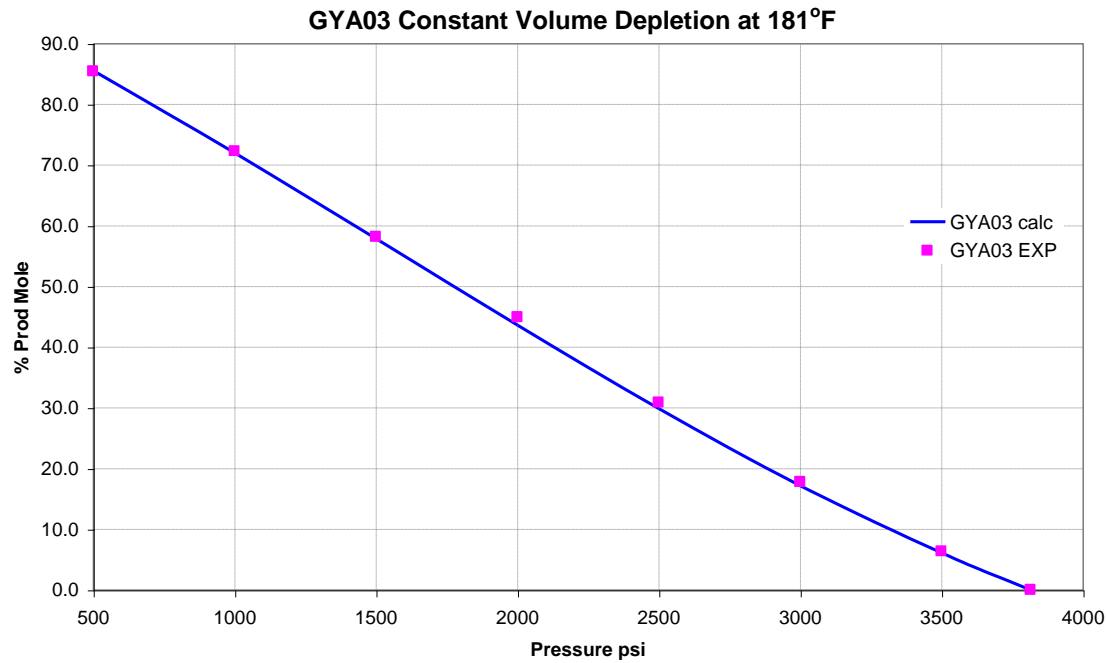


Figure 4-2 Cumulative % volume of the initial wellstream produced. Match of CVD data with full characterisation

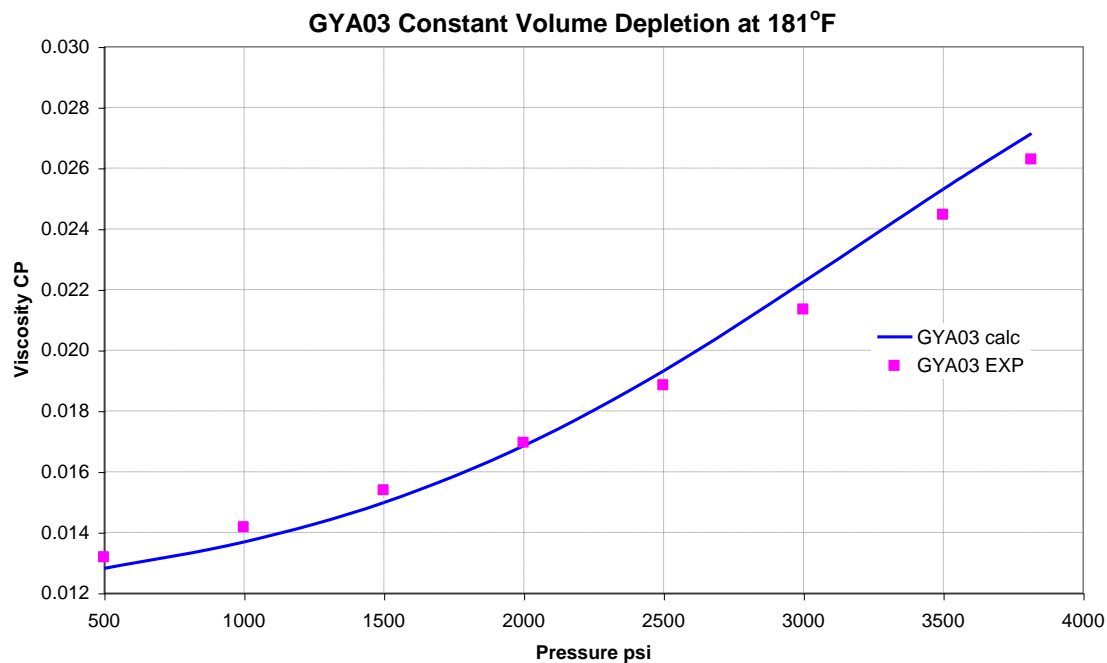


Figure 4-3 Gas viscosity (calculated) match of CVD data with full characterisation

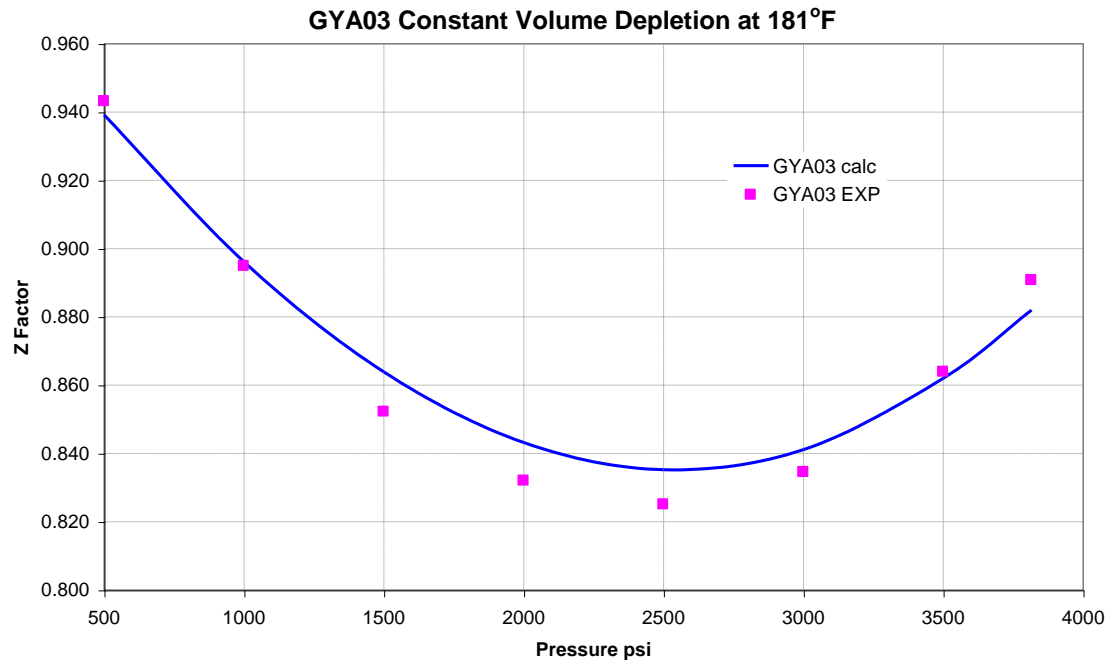


Figure 4-4 Gas compressibility Z-factor match of CVD data with full characterisation

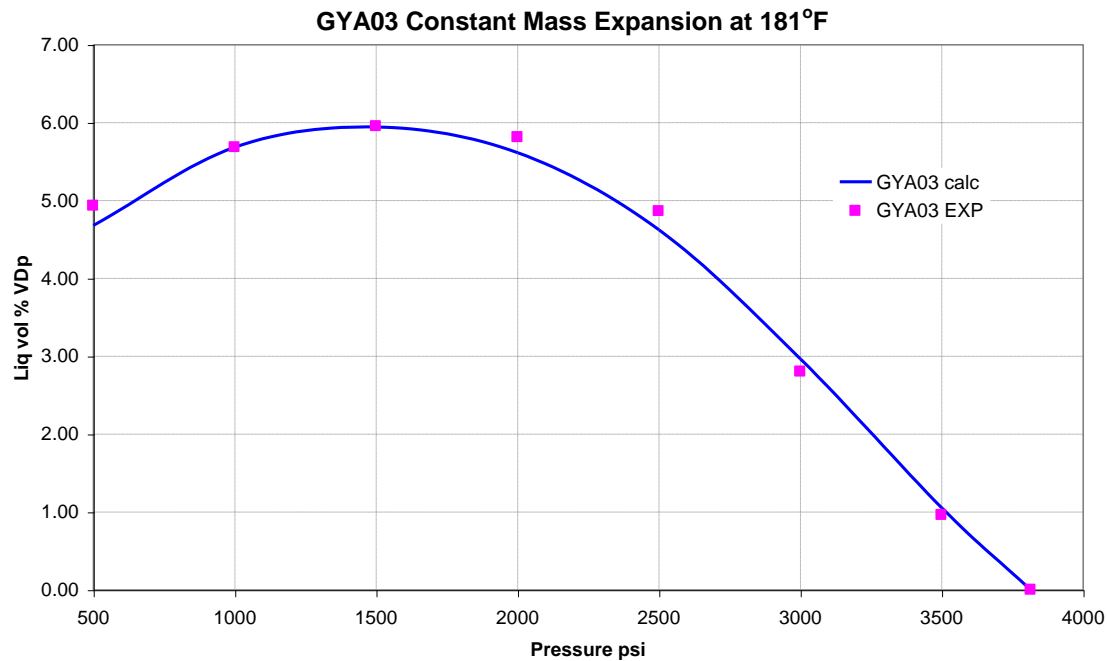


Figure 4-5 Retrograde condensate %VDp match of CME data with full characterisation

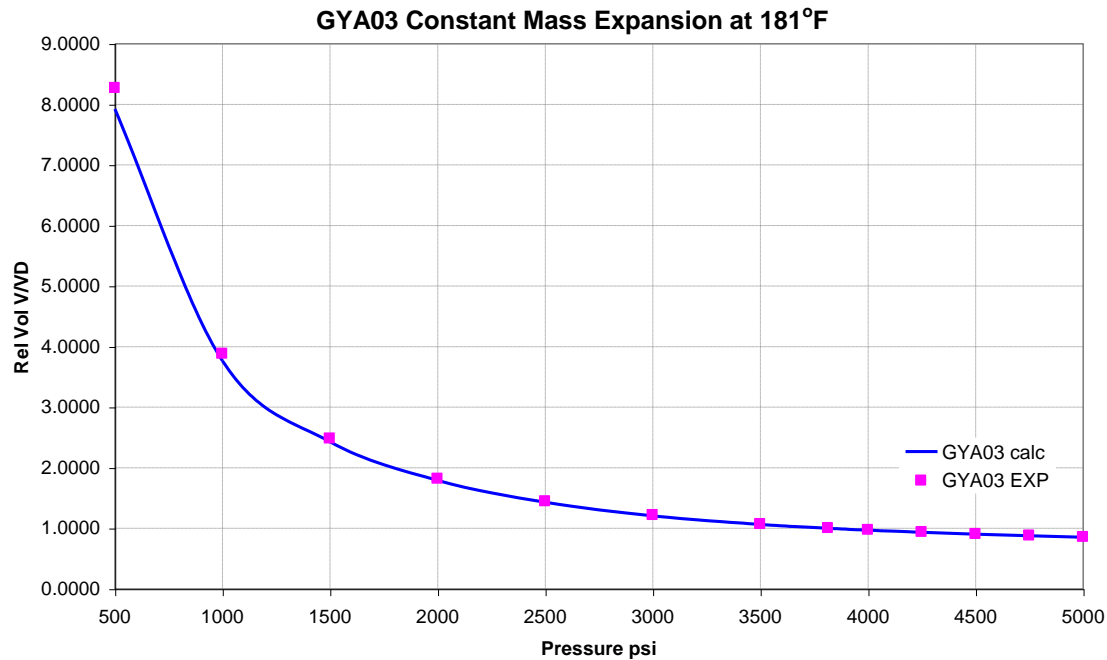


Figure 4-6 Relative volume match of CME data with full characterisation

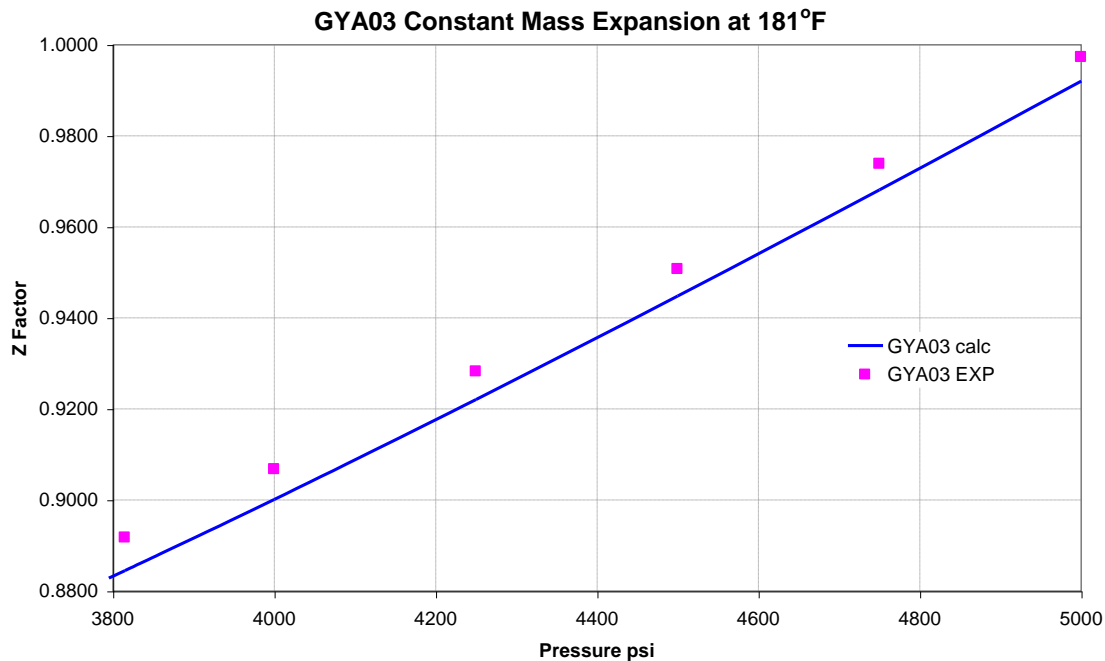


Figure 4-7 Gas deviation Z-factor match of CME data with full characterisation

The EOS characterisation was modified to improve the predictions of measured data. Nonlinear regression was used to mathematically minimize the difference between PR78P EOS predictions and measured PVT data. Adjustments of EOS parameters such as binary interaction parameters (BIPs) and heavy component critical properties were used. Interaction coefficients between C1 and C7+ pseudo-components were used to improve Saturation Pressure (Dew Point) representation. A decoupled Viscosity Experiment regression over Critical Volume on C7+ pseudo-components was used to match gas viscosity.



5. PVT lumping scheme

The original calculated recombined fluid composition determined by cryogenic distillation from GYA03 was used for the PR78P EOS calibration; components up to C20+ were included. Generally, if a sufficiently large number of pseudo-components is used to characterise the heavy fraction of a hydrocarbon mixture, a satisfactory prediction of the PVT behaviour by the equation of state can be obtained. However, in compositional models, the cost and computing time can increase significantly with the increased number of components in the system. Therefore, limitations are placed on the maximum number of components that can be used in compositional models and the original components have to be lumped into a smaller number of pseudo-components.

An initial fluid characterisation will typically contain from 13 to 20 components, and sometimes more. A stepwise pseudoisation procedure is recommended in the literature by Curtis Whitson³, whereby several pseudoised characterisations are developed sequentially (e.g. 15, 12, 10, 7, and 5 pseudo-components). The goal with each pseudoisation is to maintain PVT predictions as close to the original full characterisation as possible. With this stepwise approach, the number of pseudo-components necessary to maintain a required similarity to the original full characterisation is readily determined. Reducing the number of components in a stepwise fashion has three main advantages:

1. It is possible to establish when a further reduction in number of components results in predicted properties that deviate unacceptably from the original N-component characterisation.
2. The procedure usually results in several alternative characterisations with a common basis. One simulation might require more components than another (e.g. radial single-well study versus full-field simulation). Because several characterisations are available, and they are "related" through the original N-component characterisation, more consistency can be expected.
3. Experience has shown that better results are obtained in going from the N-component characterisation to (for example) a 7-component characterisation in several steps, than going from an N-component to a 7-component characterisation in a single pseudoisation.

For the Goldeneye case this was the approach followed. The stepwise pseudoisation procedure recommended by Whitson and presented in the following example, was followed whenever possible.

³ Whitson C.H. et al. 1999, Gas Condensate PVT – What's really important and why?, IBC Conference “Optimization of Gas Condensate Fields”, London (U.K.)



| Component | EOS22 | EOS19 | EOS12 | EOS10 | EOS9 | EOS6 | EOS4 | EOS3 |
|-----------|-------|--------|--------|--------|--------|------|------|------|
| N2 | N2 | C1N2 | C1N2 | C1N2 | C1N2 | C1N2 | | |
| CO2 | CO2 | CO2 | CO2 | CO2 | | | | |
| C1 | C1 | | | | | | | |
| C2 | C2 | C2 | C2 | C2 | | | | |
| C3 | C3 | C3 | C3 | C3 | C3 | | | |
| IC4 | IC4 | IC4NC4 | IC4NC4 | IC4NC4 | IC4NC4 | | | |
| NC4 | NC4 | | | | | | | |
| IC5 | IC5 | IC5NC5 | IC5NC5 | IC5NC5 | IC5NC5 | | | |
| NC5 | NC5 | | | | | | | |
| C6 | C6 | C6 | C6 | C6 | C6 | | | |
| C7 | C7 | C7 | | | | | | |
| C8 | C8 | C8 | | | | | | |
| C9 | C9 | C9 | | | | | | |
| C10+ | F1 | F1 | C9F1F2 | | | | | |
| | F2 | F2 | | | | | | |
| | F3 | F3 | | | | | | |
| | F4 | F4 | F3-F5 | | | | | |
| | F5 | F5 | | | | | | |
| | F6 | F6 | F3-F8 | F3-F8 | F3-F8 | | | |
| | F7 | F7 | F6-F8 | | | | | |
| | F8 | F8 | | | | | | |
| | F9 | F9 | F9 | F9 | F9 | F9 | F9 | F9 |

Figure 5-1 Example pseudoisation procedure reducing an original EOS characterisation with 22 components to multiple pseudoised characterisations [from Whitson, 1999]⁴

The original GYA03 composition was described up to C36+ and was reduced down to six pseudo-components. The following figures show the changes in phase behaviour, saturation pressure and retrograde condensate percentage from the CVD experiment, after every grouping step. It is important to see how there are minimal changes in most of the lumping stages and only at the last pseudoisation step, where the fluid characterisation was reduced from eight to six components respectively, is there any significant variation (light blue line in Figure 5-2). However, it is possible to refine by regression (fine tuning) of the newly created pseudo-components, so that the EOS predictability is maintained after the component reduction (grey line in Figure 5-2).

⁴ Whitson C.H. et al. 1999, Gas Condensate PVT – What's really important and why?, IBC Conference “Optimization of Gas Condensate Fields”, London (U.K.)

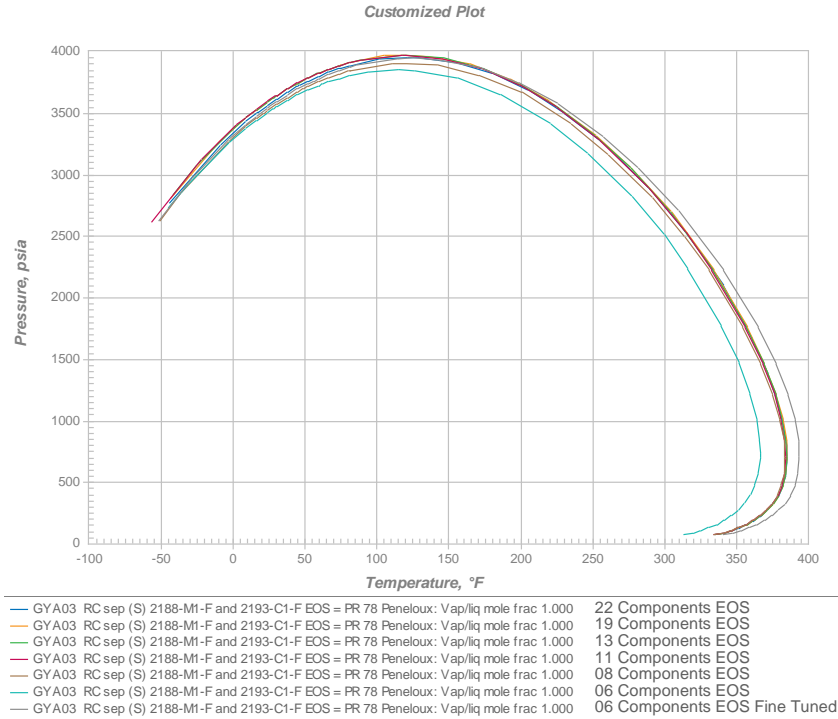


Figure 5-2 Changes in the phase envelope during the stepwise pseudoisation

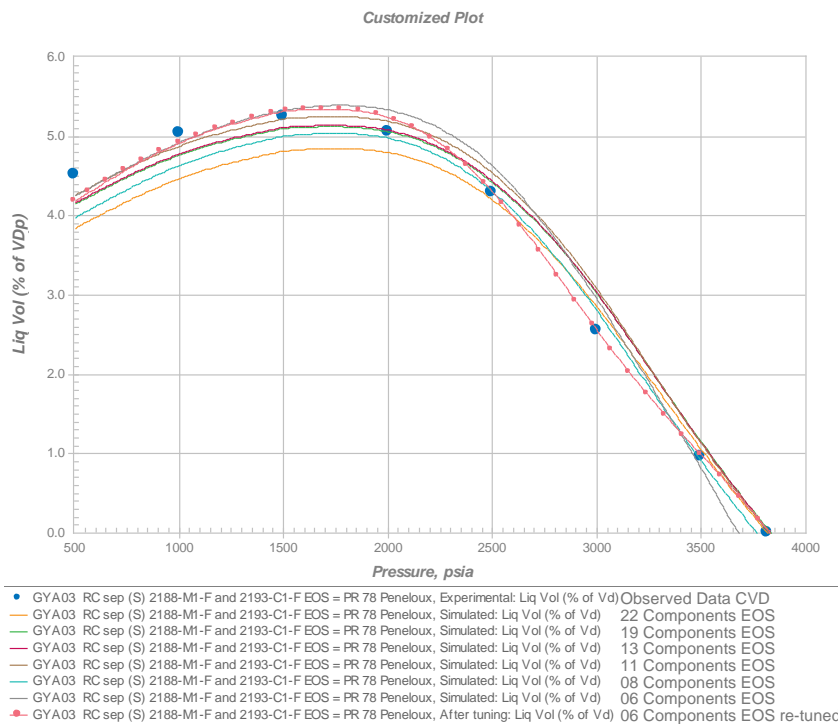


Figure 5-3. Changes in the retrograde condensate % (Vd) during the stepwise pseudoisation

The fine-tuning of the EOS restored the prediction of the phase behaviour and the changes in the retrograde condensate percentage. Now that the lumping scheme had been implemented with coherent results, it was possible to decouple the viscosity experiment and do a final regression over



the critical volume for each component's contribution to the total viscosity to match the calculated gas viscosity (from Gonzalez, Lee and Eakin 1996 ⁵). The results can be seen in the following figure.

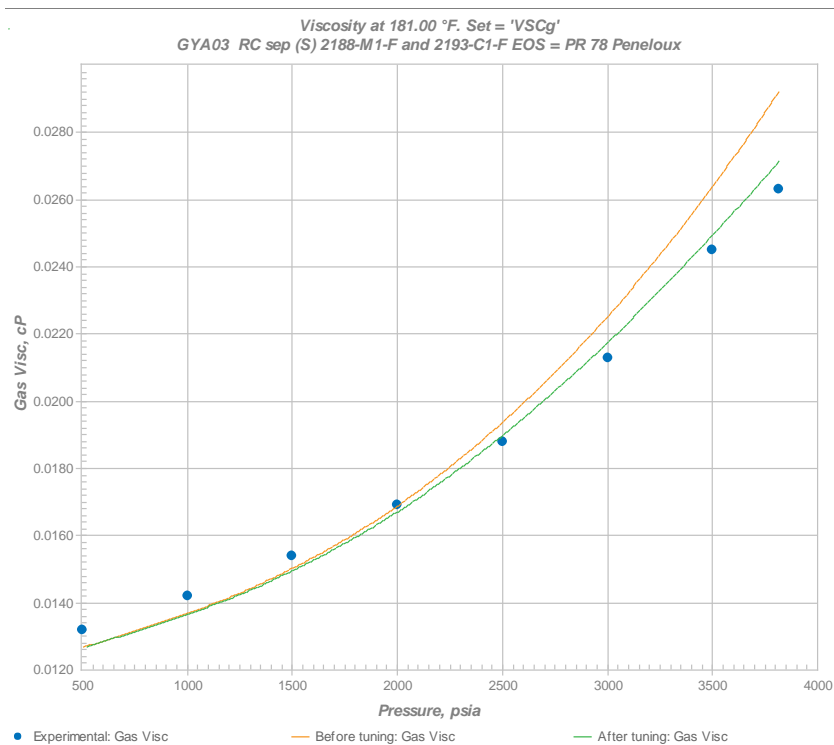


Figure 5-4. Gas viscosity before and after regressing over the critical volume

The following figure shows the mol% of the original GYA03 calculated recombined fluid composition and the resulting pseudisation lumped into six pseudo-components.

⁵ Gonzalez, Lee and Eakin 1996: "The viscosity of natural gases", J.P.T.

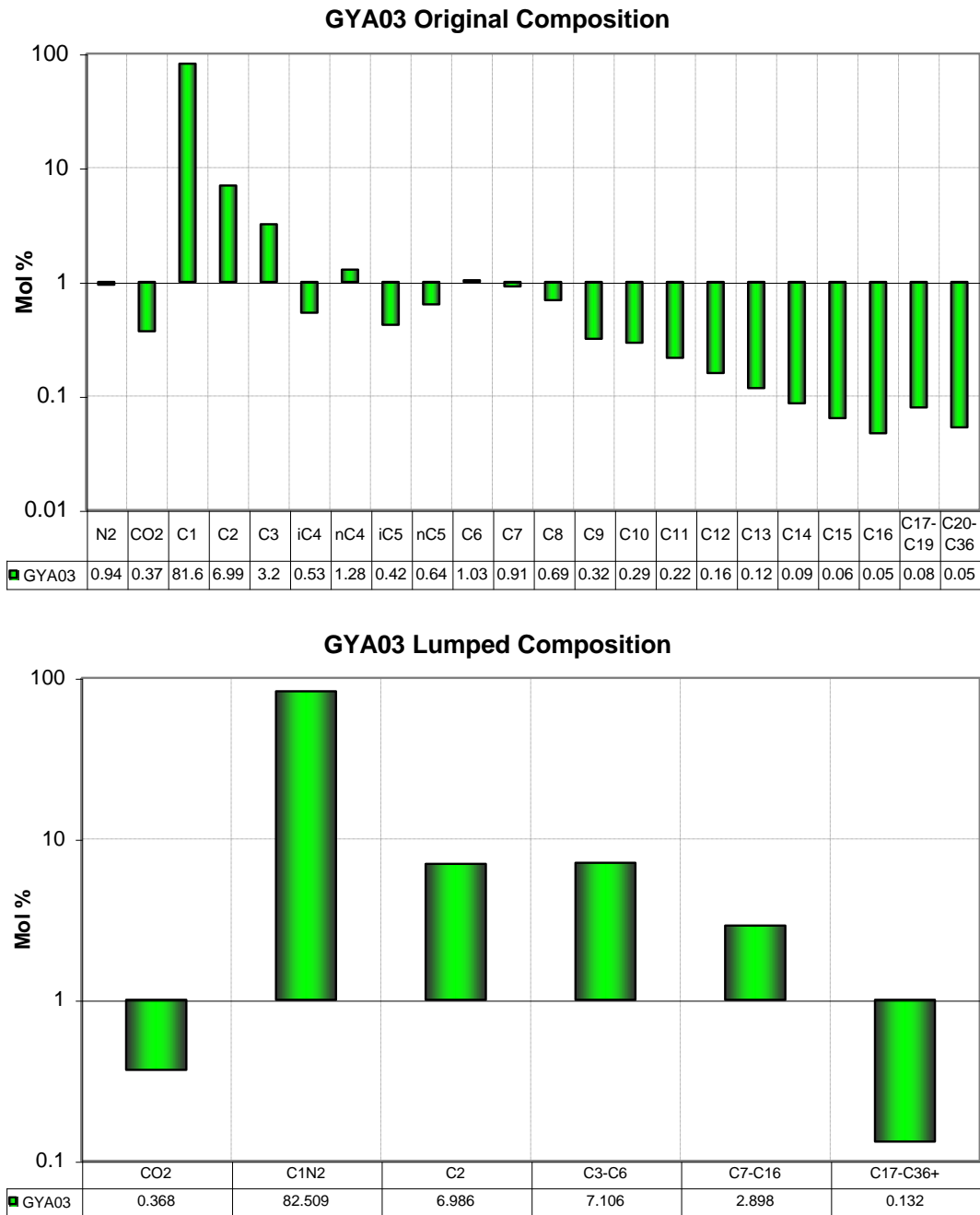


Figure 5-5. GYA03 fluid composition before and after lumping

This lumping scheme is a solution to achieve a manageable fluid characterisation for modelling the displacement processes in Goldeneye CO₂ storage. This characterisation is expected to be applicable in the majority of cases, however, further simplification might be warranted when investigating sensitivities where the mixing of CO₂ and hydrocarbon fluids is insignificant, but where significant increases in the number of grid blocks is required.



6. CO₂ fluid properties

Depleted oil and gas reservoirs are promising targets for carbon sequestration by direct carbon dioxide (CO₂) injection because of their available volume and proven integrity against leakage. The ability to simulate accurately the supercritical CO₂ and hydrocarbon properties is essential for modelling reservoir processes under injection by CO₂.

Most phenomena related to CO₂ dynamics become apparent with an understanding of the key fluid properties and their dependence on temperature and pressure.

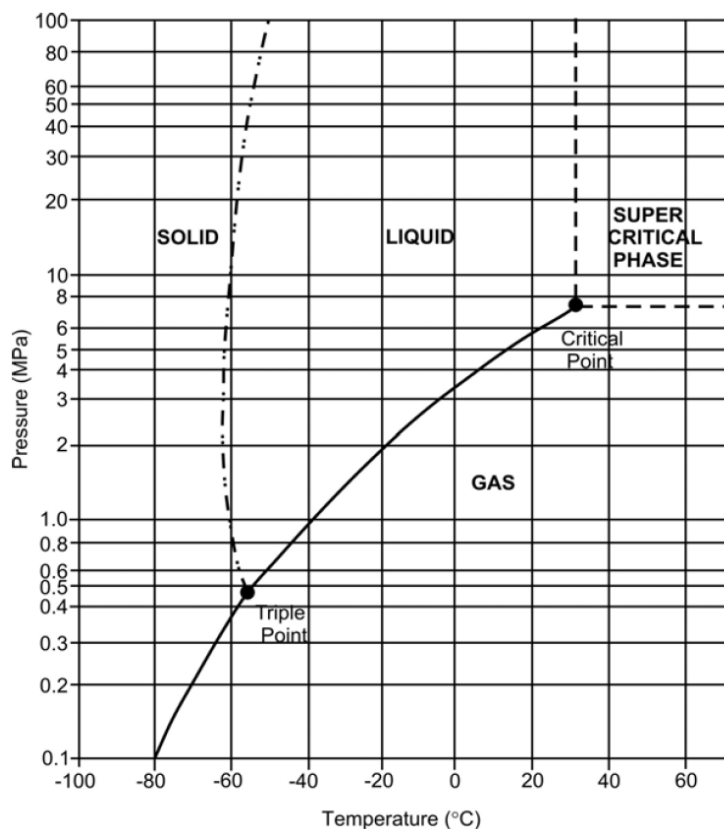


Figure 6-1. Phase diagram of CO₂ [from Wong, 2005]⁶

The critical temperature of CO₂ is 31.1° C and the critical pressure is 73.8 bar. At temperatures and pressure above this critical point, CO₂ exists as a supercritical fluid, whereby it has a density similar to a liquid but exhibits gas-like viscosity (and compressibility) (Figure 6-1).

Pure component CO₂ properties were calculated using the Thermophysical Properties of Fluid Systems from the National Institute of Standards and Technology (NIST). (<http://webbook.nist.gov/chemistry/fluid>). These properties were later used as observation points to test the predictions of the Peng-Robinson version 1978 Equation of State in its volume shift corrected Peneloux version.

The standard EOS descriptions used in reservoir simulation were developed for hydrocarbon systems and can be less accurate for modelling CO₂ properties and some other non-hydrocarbon components such as H₂S and SO₂. As a consequence, the default pure component parameters require tuning to

⁶ Wong, S.: "Module 4 – CO₂ Compression & Transportation to Storage Reservoir". APEC Reference #205-RE-01.3, 2005.



assure the best possible match over a range of interest. A set of comparison plots was prepared in order to assess the magnitude of tuning needed.

The analysis was carried out under Goldeneye reservoir conditions at an isothermal reservoir temperature of approximately 181 °F [82.78 °C] and for a pressure range that covers the probable abandonment pressure (~2000 psia [138 bara]) up to reservoir initial conditions of about 3835 psia [~264 bara].

CO₂ physical properties that strongly affect flow and transport are density (ρ), viscosity (μ), and solubility of CO₂. CO₂ dissolution in brine will be modelled using Henry's Law, whilst density is calculated directly from the EOS, and viscosity in this case calculated from the Lohrenz-Bray-Clark correlation. The following figure shows the differences between experimental data from NIST and that estimated in PVTsim through the EOS using the default pure component parameters.

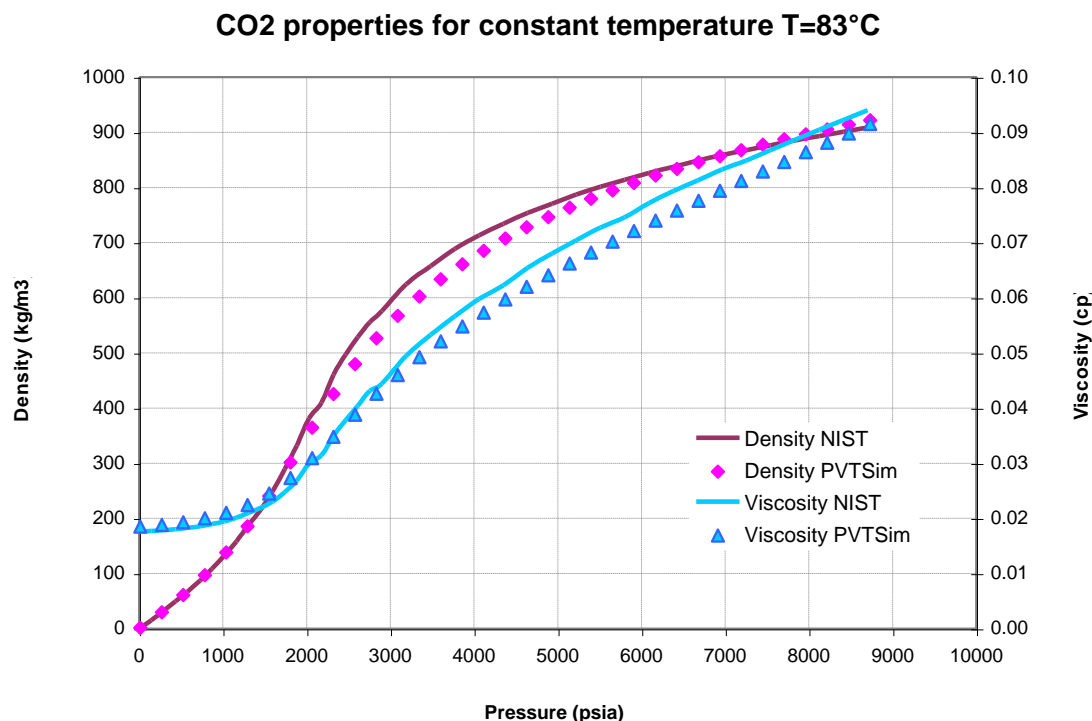


Figure 6-2. CO₂ Density and Viscosity as a function of pressure. NIST data vs. PVTsim PR78P EOS

The comparison between NIST and PVTsim shows some differences in CO₂ physical properties especially in the range of pressure that Goldeneye will operate (2000 – 3830 psia [138-246 bara]). Over this range PVTsim through PR78P EOS overestimates both CO₂ density and viscosity. The following figures show the error percentage between the two sources (PVTsim / NIST) for a range of pressures and temperatures for the default pure component EOS parameters. The light blue thicker line represents 80 °C, near Goldeneye reservoir temperature.

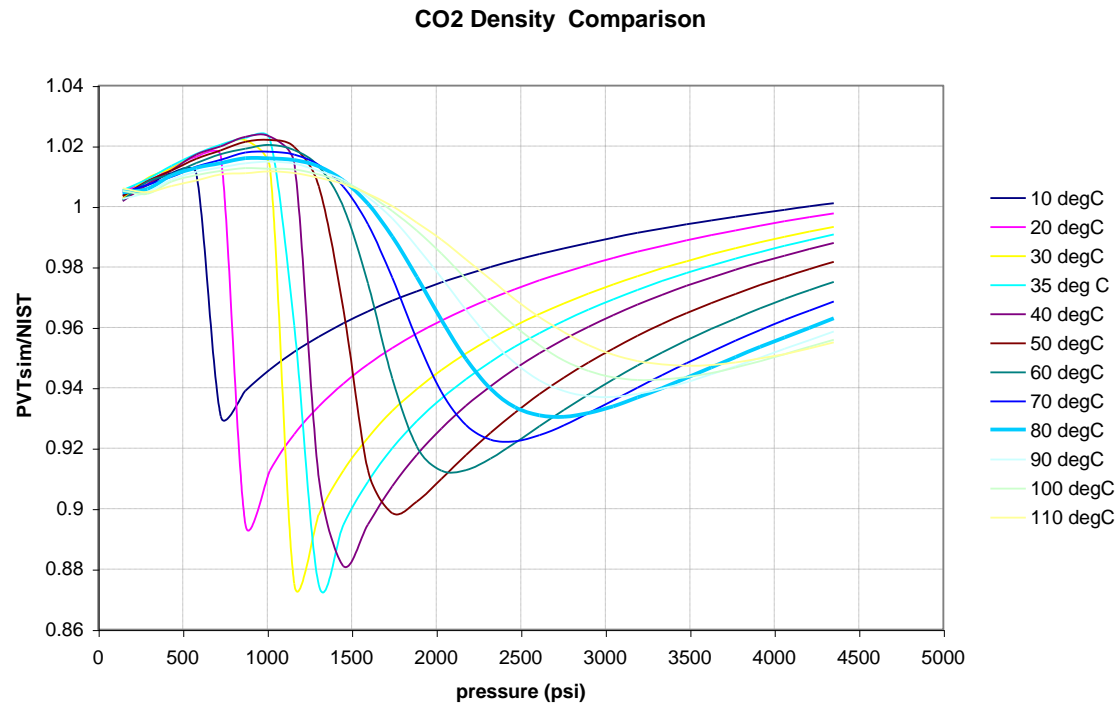


Figure 6-3. CO₂ density error function versus pressure (psia) for a range of temperatures

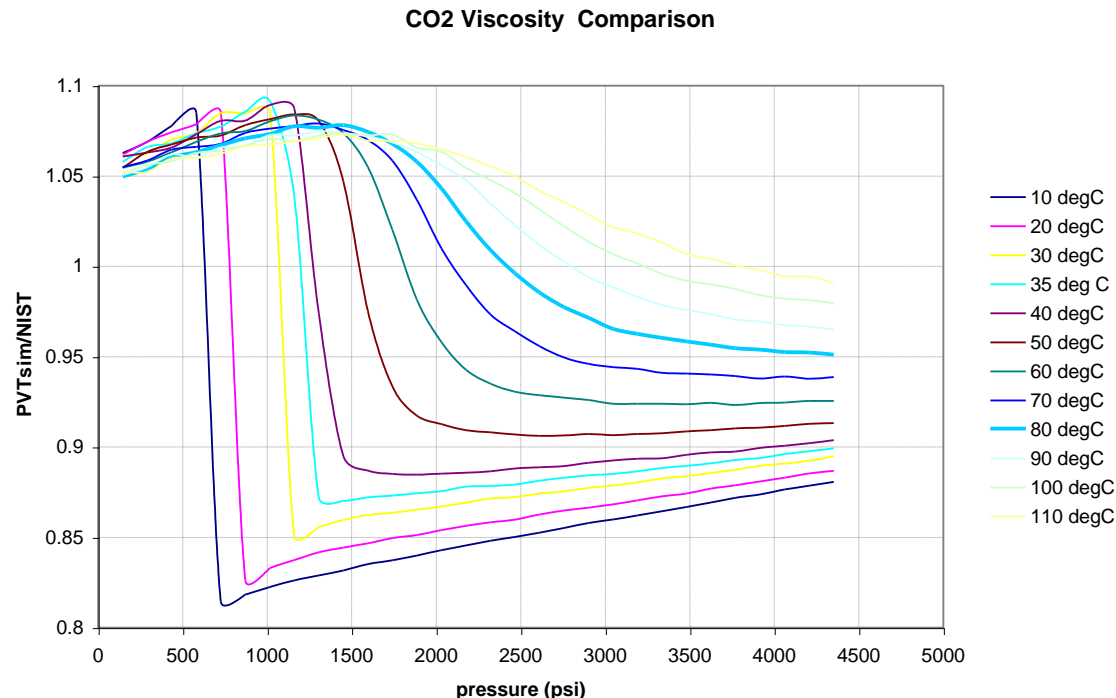


Figure 6-4. CO₂ Viscosity error function versus pressure (psia) for a range of temperatures

At Goldeneye reservoir conditions, the error in CO₂ density could be as much as 7% while in viscosity only 4.5%.



As previously discussed, issues with EOS predictions of liquid density and other fluid properties, particularly in the vicinity of the critical region, are well documented. The drawback is that the critical compressibility factor takes on a universal critical compressibility of 0.307 for all substances. Consequently, the molar volumes are typically overestimated and hence, densities are underestimated. Peneloux et al. developed a procedure for improving the volumetric predictions of EOS by introducing a volume correction parameter c_i into the equation. This third parameter does not change the vapour-liquid equilibrium conditions determined by the unmodified equation, i.e., the equilibrium ratio K_i , but modifies the liquid and gas volumes. This methodology is known as the volume translation method and was used in the CO_2 density calculation depicted previously.

This methodology has been implemented successfully on previous occasions in the prediction of the behaviour of naturally occurring hydrocarbon systems. However as has been shown previously, CO_2 is a particular component with very specific behaviour for a given set of pressure and temperature conditions. Even though the default values for volume translation for pure component CO_2 have been used, these do not always improve the calculation of density, especially where CO_2 is in a dense phase under critical or super critical conditions.

It was decided to regress over the CO_2 volume shift parameter (C_{pen} after Peneloux) in order to minimize the error between PR78 Peneloux EOS and NIST. The following figures show the impact of C_{pen} values in CO_2 density prediction.

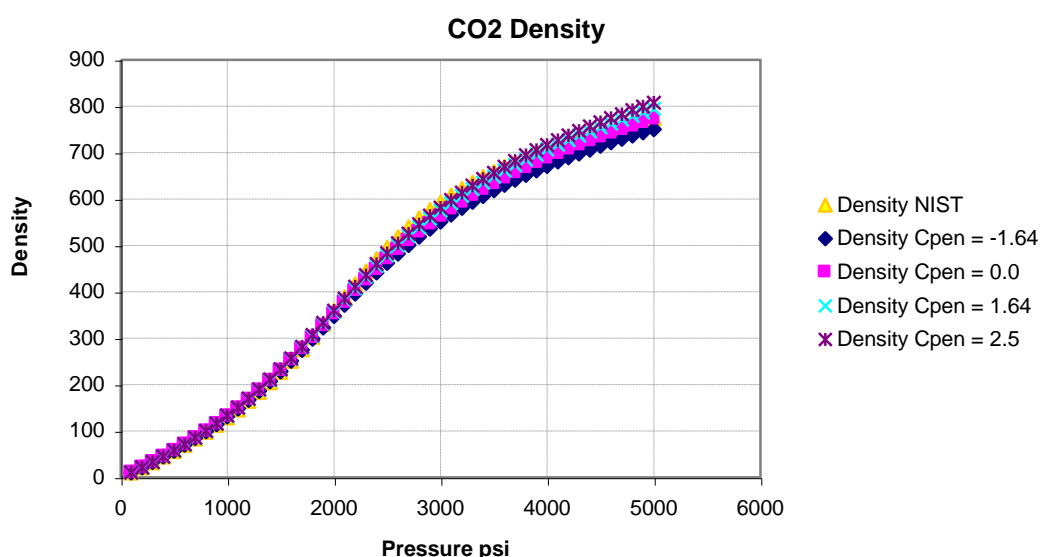


Figure 6-5. CO_2 density comparison among NIST and different volume shift values (C_{pen}) for PR78 Peneloux EOS

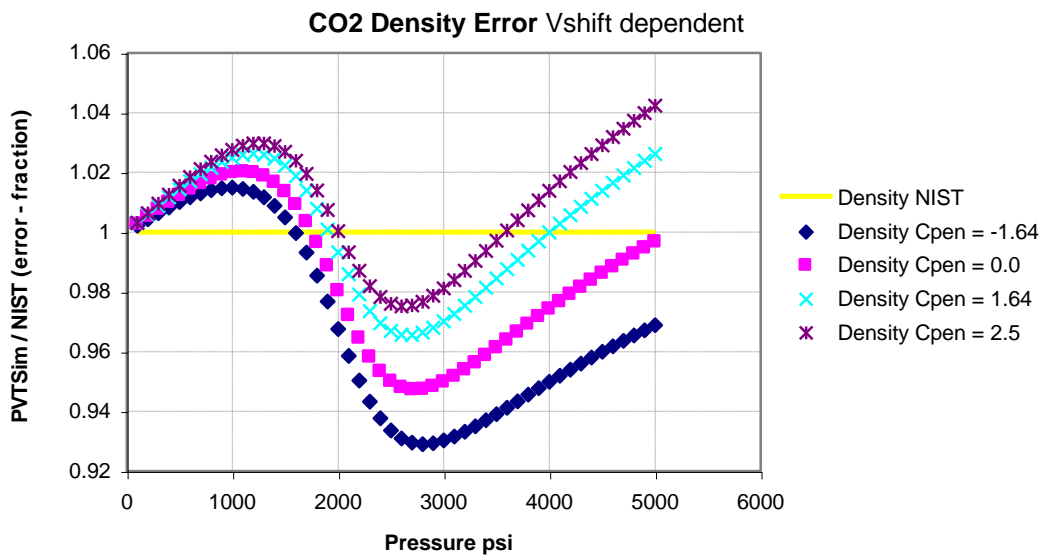


Figure 6-6. CO₂ Density error function versus pressure (psia) for a range of Copen values

It may be seen that modifying the value of volume shift parameter (C_{pen}) reduces the error between NIST and EOS, but nevertheless there is an error pressure dependency that cannot be corrected completely. Adjusting C_{pen} from $-1.64 \text{ cm}^3/\text{mol}$ to a higher value of $2.5 \text{ cm}^3/\text{mol}$ yields a better match against the NIST data, reducing the error to 2.5% in the pressure range of interest (2000 – 3835 psia [138-254 bara]). This makes CO₂ slightly less dense than the NIST data. This is a conservative assumption for the CO₂ modelling, meaning that the plume will spread further away in the same proportion.

Viscosity is calculated using the Lohrenz-Bray-Clark correlation which relates it to a fourth-degree polynomial in the reduced density, $\rho_r = \rho/\rho_c$. Sensitivities in the Volume Shift affects both CO₂ density and as a consequence, viscosity of CO₂. The following figures show the impact.

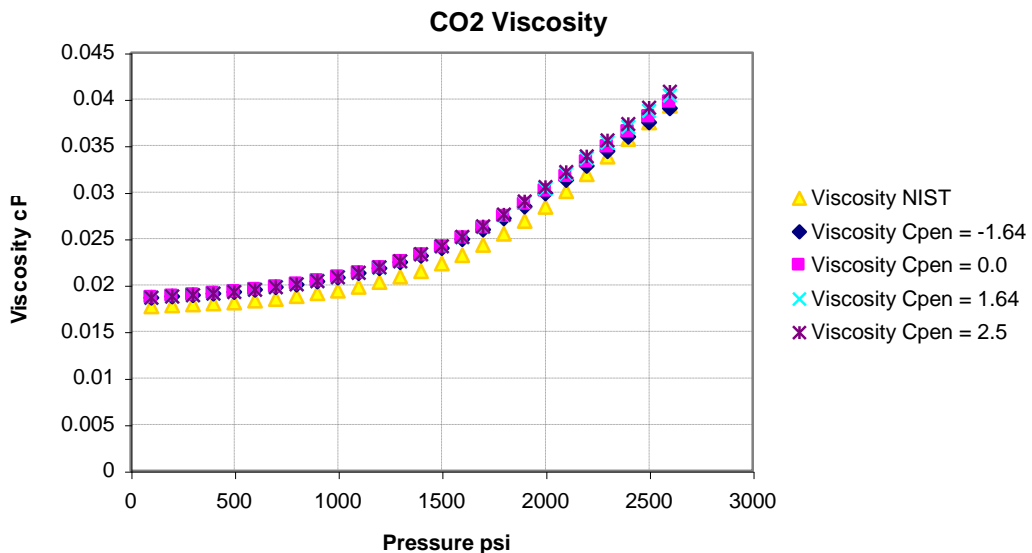


Figure 6-7. CO₂ viscosity comparison among NIST and different volume shift values (Copen) for PR78 Peneloux EOS

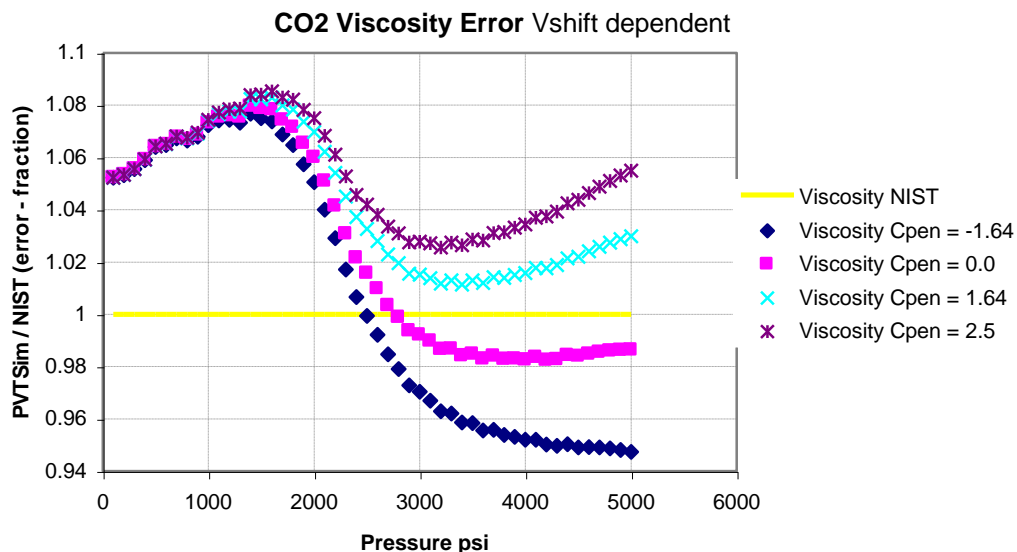


Figure 6-8. CO₂ Viscosity error function versus pressure (psia) for a range of Copen values

It may also be seen that modifying the value of volume shift parameter (C_{pen}) reduces the error between NIST and EOS, and the same pressure dependency of the error is seen in viscosity. Adjusting C_{pen} from $-1.64 \text{ cm}^3/\text{mol}$ to a higher value of $2.5 \text{ cm}^3/\text{mol}$ will increase the error up to 7.5% at low pressure (2000 psia [138 bara]).

In order to obtain a balance between the error in density and viscosity, a mid value of C_{pen} has been chosen. A value of $C_{pen} = 1.64 \text{ cm}^3/\text{mol}$ offers a mid-point between benefits, allowing a reduction of the density error from 7% to 3.2%, while maintaining viscosity error at around 2.5% in average for the pressure range of interest.

It is important to understand that these differences in CO₂ viscosities are small in comparison with the range of uncertainty of other parameters such as the relative permeabilities.

When outputting the gas condensate EOS model from PVTsim in “simulator”, the volume shift parameters (C_{pen}) for the CO₂ component are modified as described above.

7. Conclusion

Effective modelling of the Goldeneye hydrocarbon reservoir fluids and the injected CO₂ properties is achievable using a Peng-Robinson equation of state representation, lumped into six components. The densities and viscosities are modelled using the Peneloux correlation adjunct to the PR EOS, and the C_{pen} factor has to be tuned to yield correct CO₂ properties at storage conditions.



8. Abbreviations

| | |
|------------------|--|
| BIP | Binary Interaction Parameters, also known as Binary Interaction Coefficients (BIC) |
| CCS | Carbon, Capture and Storage |
| CME | Constant Mass Expansion, also known as Constant Composition Expansion (CCE) |
| CO ₂ | Carbon Dioxide |
| C _{pen} | Volume Shift Parameter after Peneloux |
| CVD | Constant Volume Depletion |
| D _p | Dew Point |
| DST | Drill Stem Test |
| EOS | Equation of State |
| H ₂ S | Hydrogen sulphide |
| LBC | Lohrenz-Bray-Clark |
| MDT | Modular Dynamic Tester |
| NIST | National Institute of Standards and Technology |
| P&T | Pressure and Temperature |
| PR | Peng-Robinson |
| PVT | Pressure, Volume and Temperature |
| RFT | Repeat Formation Tester |
| SO ₂ | Sulphur dioxide |
| VD _p | Volume at Dew Point |

In the text well names have been abbreviated to their operational form. The full well names are given in Table 8-1 below.

Table 8-1 Well name abbreviations

| Full well name | Abbreviated well name |
|----------------|-----------------------|
| DTI 14/29a-A3 | GYA01 |
| DTI 14/29a-A4Z | GYA02S1 |
| DTI 14/29a-A4 | GYA02 |
| DTI 14/29a-A5 | GYA03 |
| DTI 14/29a-A1 | GYA04 |
| DTI 14/29a-A2 | GYA05 |